Signatures of the light gluino in top quark production

Chong Sheng Li*
Department of Physics, Peking University, Beijing 100871, China

P. Nadolsky† and C.-P. Yuan‡
Department of Physics and Astronomy, Michigan State University, East Lansing, Michigan 48824

Hong-Yi Zhou§
Institute of Modern Physics and Department of Physics, Tsinghua University, Beijing 100084, China

(Received 9 April 1998; published 22 September 1998)

If a light gluino, with a mass of the order of GeV, exists in the minimal supersymmetric extension of the standard model, then it can contribute to the production rate of the top quark pairs at hadron colliders via $\tilde{g}\tilde{g}\to t\bar{t}$. Because the top quark is heavy, the masses of the superpartners of the left-handed and right-handed top quarks can be very different such that a parity-violating observable can be induced in the tree level production process. We discuss the phenomenology of this parity violating asymmetry at the CERN Large Hadron Collider. [S0556-2821(98)02819-7]

PACS number(s): 12.60.Jv, 13.88.+e, 14.80.Ly

I. INTRODUCTION

Despite the success of the standard model (SM) in explaining and predicting experimental data, it is widely believed that new physics has to set in at some high energy scale. One of such new physics models is the minimal supersymmetric extension of the standard model (MSSM) [1]. Various supersymmetry (SUSY) models, such as gravity-mediated and gauge-mediated supersymmetry breaking models [2], have been extensively considered in the literature to explain why the masses of the superparticles are not the same as those of the SM particles. In general, the masses of the superparticles are predicted to be around a few hundred GeV or at the TeV region. There are ample studies in the literature which examine the detection of these nonstandard particles in current and future experiments, including those at the CERN Large Hadron Collider (LHC), and at the future linear colliders.

Among the superparticles of the MSSM, some models of SUSY breaking predict the existence of a light gluino with a mass around 1 GeV or less [3]. If this scenario is true, then there is rich phenomenology predicted for the current experimental data which can be used to either confirm or constrain models. In Ref. [4], the ALEPH Collaboration used the data on the cross sections of dijet production and the angular distributions in four-jet production to derive the ratios of the color factors C_A/C_F and T_F/C_F. Based on the obtained values, ALEPH excluded the existence of gluinos with a mass lighter than 6.3 GeV at the 95% confidence level. The result was criticized by Farrar [5], who argued that ALEPH's analysis underestimated the theoretical uncertainties in the knowledge of hadronization and resummation of large logarithms arising in the separation of jets from soft radiation. If these uncertainties are taken into account, the light gluino is excluded only at the 1σ level. This problem was further examined by Csikor and Fodor in Ref. [6], where they determined the color factors of underlying gauge theory by studying the behavior of the ratios $R_\gamma=\sigma(e^+e^-\to\text{jets})/\sigma(e^+e^-\to\mu^+\mu^-)$, $R_\tau=\Gamma(\tau^-\to\nu_\tau+\text{jets})/\Gamma(\tau^-\to\nu_\tau e^-\overline{\nu_e})$, $R_Z=\Gamma(Z\to\text{hadrons})/\Gamma(Z\to\mu^+\mu^-)$ in the region of 5 GeV to the M_Z scale. They concluded that the $\mathcal{O}(\alpha_s^3)$ analysis of these quantities allows one to exclude light gluinos with a mass between 3 and 5 GeV at the 93% confidence level, and with a mass less than 1.5 GeV at the 70.8% confidence level. If their results are combined with the χ^2 distribution from ALEPH analysis, the exclusion confidence level is improved to 99.97 and 99.89%, respectively. This conclusion is quite insensitive to the overall error of ALEPH's results; for instance, the exclusion limits of the combined analysis are still above 95% if ALEPH's systematic error is increased by a factor of 3. However, in order to extract the number of active fermions from the experimental data, both methods of [4] and [6] rely on the state-of-art usage of perturbative theory. Neither of the analyses can exclude the light gluino at the confidence level $\geqslant 70\%$, and a combined and complicated analysis is needed to overcome the flaws of each method.

Another significant limitation on the possible parameter space of the models with light gluinos was recently imposed by the negative results of the search for the production of charginos with a mass less than the m_W at the CERN e^+e^- collider LEP2 [7]. This result disfavors the models with the masses of all gauginos vanishing at the tree level at the grand unified theory (GUT) scale [3], in which the gluino has a mass of the order GeV at the electroweak scale, and at least one of the charginos is necessarily lighter than the W boson. However, the LEP2 data cannot rule out models with the other spectra of gaugino masses, for instance, the models of gauge-mediated symmetry breaking where the gluino can be the only light gaugino [8]. As mentioned before, the analysis

*Electronic address: csli@pku.edu.cn
†Electronic address: nadolsky@pa.msu.edu
‡Electronic address: yuan@pa.msu.edu
§Electronic address: hongyi@thphys.uni-heidelberg.de

of Refs. [4,6] already puts strong constraints on the possibility of the light mass of the gluino, however, due to the aforementioned theoretical difficulties it seems that more study is needed.

There are a few other methods discussed in the literature to look for light gluino. If the gluino is light and hadronizes before reaching the detector, it should be possible to observe its bound states, for example, R^0 mesons, created by the binding of a gluon and gluino [9]. Although the region of R^0 masses is significantly restricted by KTeV measurements [10], R^0 can still exist in the mass region 1.4–2.2 GeV [11].

If the squark masses are of the order of several hundreds GeV, the light mass of the gluino can lead to noticeable peaks in the dijet invariant mass and angular distributions at the Fermilab Tevatron or LHC, arising due to the resonant production of massive squarks in quark-gluino fusion [12]. The already existing Tevatron data allows to exclude light gluino models with masses of the lighter squarks lying between 150 and 650 GeV [12]; it would be desirable to continue the search for the resonant peaks at Tevatron, as well as at LHC, where the increased dijet production cross section would allow to cover a larger region of squark masses.

In perturbative QCD (PQCD) theory, the existence of a light gluino would change the running of the strong coupling, as well as the form of the Dokshitzer-Gribov-Lipatov-Altarelli-Parizi (DGLAP) equations. Therefore, to describe the existing deep inelastic scattering (DIS) data, it is necessary to account not only for the quark and gluon distribution functions inside the initial hadron(s), but also for the gluino distribution which has different renormalization group properties. An obvious question is whether the currently available hadronic data is consistent with the existence of a light gluino. The last analysis of this type was done in Refs. [13,14], which showed that the existence of the light gluino did not contradict DIS data available at that time. However, those analyses did not include the more recent data from H1, ZEUS, and New Muon Collaboration (NMC) experimental groups [15–17] covering the region of lower x and Q^2. These new data can be crucial for testing the scenario of having a light gluino in supersymmetry models, because the existence of a light gluino would imply a slower running of the parton distribution functions from low to high Q^2.

The existence of new types of particle interactions can be proved if one observes the violation of the symmetries of the standard model, for instance, the significant violation of the discrete symmetry with respect to space reflections (P parity) in strong interactions. An experimental search for parity-violating effects could be performed relatively easy in processes with t quarks in the final state, due to the possibility of tracing the polarization of the top quarks decaying through the channel $t \to W^+ + b$. Therefore, in this work we would like to concentrate on the production of top quark pairs. For the top quark pairs produced at hadron colliders, the SM allows the production processes $q\bar{q}, GG \to G \to t\bar{t}$ to violate P parity in next-to-leading orders due to the presence of W and Z bosons in the loop diagrams. However, this effect is shown to be negligible [18]. On the other hand, for certain choices of SUSY parameters in the MSSM, it is possible to obtain a large difference between the masses of right-top squarks and left-top squarks, which in principle can lead to some noticeable asymmetries in the production of right- and left-handed top quarks. These asymmetries arise either in the next-to-leading order of the SUSY QCD process $q\bar{q}, GG \to G \to t\bar{t}$, or at the tree level of the SUSY QCD process $\tilde{g}\tilde{g} \to t\bar{t}$. The asymmetries of the first type were studied earlier in Ref. [19]. It was shown that at Tevatron the difference in the cross sections of right- and left-handed t-quark production can be of the order 2–3% provided the right-top squark is light. This conclusion holds for a wide range of gluino masses. As will be shown below, the asymmetries of the second type can only be noticeable if gluinos are light, and the parton density of gluinos in the nucleon is comparable with that of the sea quarks.

The primary goal of this article is to present the leading order (LO) study of the second scenario, and to evaluate the impact of the small mass of gluino on the production of t quarks at the CERN Large Hadron Collider. In the first part of this study we obtain the LO distributions of the partons in the nucleon taking in to account the possible nonzero contents of light gluinos. For this purpose we modified the fitting program used previously to obtain CTEQ4L parton distributions [20]. Since we present the leading order calculation, we considered it sufficient not to perform the complete NLO analysis of parton distributions, contrary to what was done in Refs. [13, 14].

In the course of this study, it was a surprise for us to find that the account for the new hadronic data from H1, ZEUS, and NMC groups [15–17], which was not available at the time of the previous studies [13,14], tends to increase the overall χ^2 of the fit after the inclusion of a light gluino. The reason for this is that these new data cover the region of lower x and Q^2, thus making the analysis more sensitive to the slower running of the parton distributions in SUSY QCD theory with a light gluino. Nonetheless, we would like to be extremely cautious about this observation and refrain from any final conclusions about the consistency of the current experimental data and SUSY QCD theory with a light gluino before a more thorough next-to-leading order global analysis of hadronic data is made. Instead, we would like to concentrate on the primary goal of this paper, namely, on the calculations of the top quark production asymmetries at the LHC. For this process, the Bjorken x of the initial state partons are allowed to lie in the range

$$\frac{4m_t^2}{s} = 6.25 \times 10^{-4} \leqslant x_{1,2} \leqslant 1, \tag{1}$$

where the parton distributions are less dependent on the low x data. We therefore expect the results of this work to be stable with respect to the possible changes in the parton distributions, and that these changes will not introduce an uncertainty more important than those coming from other sources (e.g., next-to-leading order corrections).

After obtaining the parton distribution functions (PDFs) in SUSY QCD theory with a light gluino, we calculate the degree of parity violation in the $t\bar{t}$ pairs produced via the LO $\tilde{g}\tilde{g} \to t\bar{t}$. Thus, the paper consists of three main sections: the

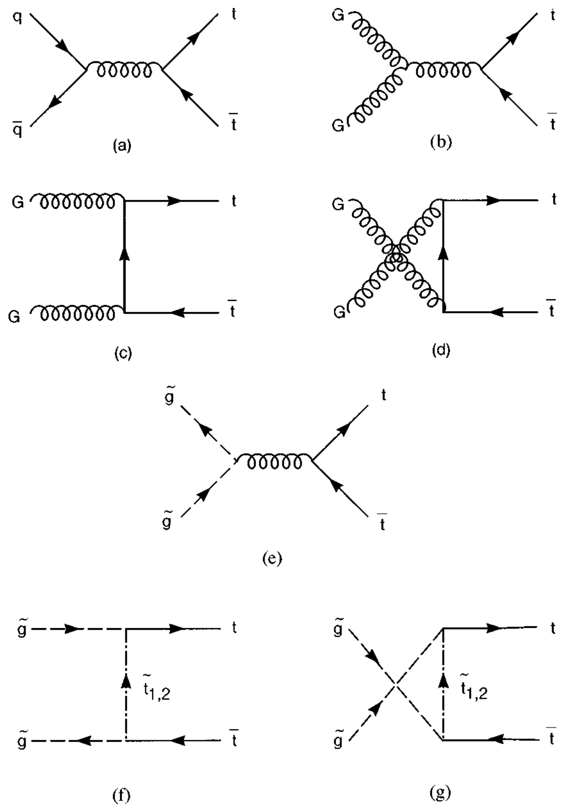

FIG. 1. Leading order diagrams contributing to the production of top quarks in SUSY QCD theory.

description of the parton distribution functions for SUSY QCD theory with a light gluino, the calculation of the cross sections for the process $pp(\tilde{g}\tilde{g})\to t_{L,R}\overline{t}$, and a numeric analysis of the asymmetries in left- and right-handed top quark production. Finally, the conclusion summarizes the obtained results.

II. PARTON DISTRIBUTIONS

We start the construction of parton distributions by assuming that the only superparticle actively present in the nucleons at the energies of the supercolliders is a gluino with a mass much smaller than the typical scales of $t\overline{t}$ production (less than 1.5 GeV compared to $m_t \approx 175$ GeV). For the purpose of our calculation, we incorporate the gluino sector into the PDF evolution package, used recently to build the set of CTEQ4 unpolarized parton distributions [20]. In order to simplify the modifications in the fitting program, we used an approach close to the one adopted by the authors of Glück-Reya-Vogt (GRV) distributions [14]. The input scale Q_0 for the parton distributions was chosen to be lower than in CTEQ4L and equal to the mass of the gluino (assumed to be $m_{\tilde{g}}=0.5$ GeV in this study, unless stated otherwise). At this scale, the only input distributions are of gluons and lighter (u,d,s) quarks, while the nonzero PDFs of gluinos and heavy quarks are radiatively generated at scales above their mass thresholds.

In the presence of a light gluino, two aspects of the leading-order evolution of parton distributions are different than those in standard QCD. First, the one-loop β function, determining the running of the strong coupling α_s,

$$\alpha_s(Q^2)=\frac{4\pi}{\beta_0 \ln(Q^2/\Lambda^2)}, \tag{2}$$

now has the form

$$\beta_0=11-\frac{2}{3}n_f-2n_{\tilde{g}}, \tag{3}$$

where n_f and $n_{\tilde{g}}$ are the number of active quark flavors and gluinos, respectively. In our analysis, we use $\alpha_s(M_Z)=0.118$ and $\Lambda=7.65$ MeV for five flavors. The matching of α_s between 4 and 5, or 5 and 6 flavors takes place at $Q=5.0$ GeV and $Q=175$ GeV, respectively, which are defined as the bottom and top quark masses.

Second, the leading order DGLAP equations should now account for the splittings $\tilde{g}\to q\tilde{\bar{q}}$, $\tilde{g}\to g\tilde{g}$, and $g\to\tilde{g}\tilde{g}$, so that the singlet equation takes the form

$$\frac{d}{dt}\begin{pmatrix} q_S(x,Q^2)\\ G(x,Q^2)\\ \tilde{g}(x,Q^2)\end{pmatrix} =\frac{\alpha_S(Q^2)}{2\pi} \times\int_x^1 \begin{pmatrix} P_{qq}(x/y) & P_{qG}(x/y) & P_{q\tilde{g}}(x/y)\\ P_{Gq}(x/y) & P_{GG}(x/y) & P_{G\tilde{g}}(x/y)\\ P_{\tilde{g}q}(x/y) & P_{\tilde{g}G}(x/y) & P_{\tilde{g}\tilde{g}}(x/y)\end{pmatrix} \times\begin{pmatrix} q_S(y,Q^2)\\ G(y,Q^2)\\ \tilde{g}(y,Q^2)\end{pmatrix}\frac{dy}{y}. \tag{4}$$

The splitting functions used in Eq. (4) can be found, e.g., in [21].

With the help of the upgraded evolution package we performed the fit of the experimental data, closely following the procedure of the construction of the CTEQ4L PDF set, as described in [20]. However, for simplicity, the fit did not use the jet data, and the value of the strong coupling was fixed to be equal to the world-average value $\alpha_s(M_Z)=0.118$. As a result, we obtained the set of parton distributions SUSYL, which was used throughout the rest of the paper.

III. CALCULATION OF THE MATRIX ELEMENTS

At the LHC, $t\overline{t}$ pairs will be dominantly produced from the standard QCD processes of $q\overline{q}$ and GG interactions, as shown in Figs. 1(a)–1(d). All of these diagrams preserve P parity. In SUSY QCD theory, if the mass of the gluino is small $(m_{\tilde{g}}\sim 1$ GeV), we will also expect a noticeable contribution due to the annihilation of gluinos, described by the three diagrams of Figs. 1(e)–1(g). The s-channel diagram of Fig. 1(e) is equivalent, up to a color factor, to the analogous $q\overline{q}$ diagram of Fig. 1(a) and does not break parity; however, the parity symmetry is broken in the t and u channels due to the mechanism of squark mass mixing which is briefly described below.

In MSSM the left squark and right squark, superpartners of the the left- and right-handed quarks, do not have a definite mass but instead are a mixture of two mass eigenstates. These mass eigenstates $\tilde{q}_1$ and $\tilde{q}_2$ are related to the current eigenstates $\tilde{q}_L$ and $\tilde{q}_R$ by

$$\tilde{q}_1=\tilde{q}_L \cos \theta_q+\tilde{q}_R \sin \theta_q, \quad \tilde{q}_2=-\tilde{q}_L \sin \theta_q+\tilde{q}_R \cos \theta_q. \tag{5}$$

Due to this, MSSM in general allows us to have nonzero asymmetries in $q\bar{q}$-pair production, defined by

$$A_q=\frac{\sigma(pp\to q_L\bar{q})-\sigma(pp\to q_R\bar{q})}{\sigma(pp\to q_L\bar{q})+\sigma(pp\to q_R\bar{q})}, \tag{6}$$

where σ denotes the cross section of $t\bar{t}$-pair production, integrated over the relevant part of the phase space to be discussed below. The best chance to observe a nonzero A_q is provided by the $t\bar{t}$ production process, where the mixing between the squarks is the largest due to the large mass of the top quark. In the following, we ignore the mass mixing for the five lighter quarks.

In the MSSM, the squark-quark-gluino interaction Lagrangian is given by

$$L_{\tilde{g}\tilde{q}\bar{q}}=-g_s T^a_{jk}\bar{q}_k[(a_1-b_1\gamma_5)\tilde{q}_{1j} +(a_2-b_2\gamma_5)\tilde{q}_{2j}]\tilde{g}_a+\text{H.c.}, \tag{7}$$

where g_s is the strong coupling constant, T^a are $\mathrm{SU}(3)_C$ generators, and a_1, b_1, a_2, b_2 are given by

$$a_1=\frac{1}{\sqrt{2}}(\cos \theta_q-\sin \theta_q)=-b_2,$$

$$b_1=-\frac{1}{\sqrt{2}}(\cos \theta_q+\sin \theta_q)=a_2. \tag{8}$$

The mixing angle θ_t and the masses $m_{\tilde{t}_1}$, $m_{\tilde{t}_2}$ can be calculated by diagonalizing the following mass matrix:

$$\begin{pmatrix} M^2_{\tilde{t}_L} & m_t m_{LR} \\ m_t m_{LR} & M^2_{\tilde{t}_R}\end{pmatrix}, \tag{9}$$

where $M^2_{\tilde{t}_{L,R}}$ and m_{LR} are the parameters of the soft-breaking terms in the MSSM.

From Eq. (9), we can derive the expressions for $m^2_{\tilde{t}_{1,2}}$ and θ_t:

$$m^2_{\tilde{t}_{1,2}}=\frac{1}{2}[M^2_{\tilde{t}_L}+M^2_{\tilde{t}_R}\mp\sqrt{(M^2_{\tilde{t}_L}-M^2_{\tilde{t}_R})^2+4m_t^2 m^2_{LR}}], \tag{10}$$

$$\tan \theta_t=\frac{m^2_{\tilde{t}_1}-M^2_{\tilde{t}_L}}{m_t m_{LR}}. \tag{11}$$

Inversely,

$$M^2_{\tilde{t}_{R,L}}=\frac{1}{2}[m^2_{\tilde{t}_1}+m^2_{\tilde{t}_2}\mp\sqrt{(m^2_{\tilde{t}_2}-m^2_{\tilde{t}_1})^2-4m_t^2 m^2_{LR}}]. \tag{12}$$

The asymmetry A_t depends on the angle of mixing θ_t in the following manner. The denominator of A_t is dominated by the large contributions from the quark and gluon channels [Figs. 1(a)–1(d)] and therefore shows little dependence on the masses of top squarks. The numerator of the asymmetry depends both on the splitting and the mixing of the squark masses. Since left-right-handed quarks couple only to left-right squarks, in the case of no mass mixing ($m_{LR}=0$) the asymmetry is completely determined by the difference of masses $M_{\tilde{q}_L}-M_{\tilde{q}_R}$. In this limit $\theta_t\approx-\pi/2$, provided that $M_{\tilde{t}_R}<M_{\tilde{t}_L}$.

For fixed mass eigenvalues $m_{\tilde{t}_{1,2}}$, the relationship (12) for the mass parameters $M_{\tilde{t}_{L,R}}$ puts the upper bound on m_{LR}:

$$m_{LR}\leqslant\frac{m^2_{\tilde{t}_2}-m^2_{\tilde{t}_1}}{2m_t}. \tag{13}$$

For largest m_{LR},

$$\theta_t=-\frac{\pi}{4} \tag{14}$$

and

$$M_{\tilde{t}_L}=M_{\tilde{t}_R}. \tag{15}$$

In this limit, top squark mass eigenstates have the maximal mixing between the left- and right-top squarks, so that the asymmetry A_t becomes zero. Thus, for fixed mass eigenstates, the asymmetries are expected to decrease with the growth of m_{LR}.

In gravity-mediated supersymmetry breaking models (MSUGRA), the masses of left- and right-top squarks satisfy the relations

$$M^2_{\tilde{t}_L}=m^2_{\tilde{t}_L}+m_t^2+\left(\frac{1}{2}-\frac{2}{3}\sin^2 \theta_W\right)\cos(2\beta)m_Z^2,$$

$$M^2_{\tilde{t}_R}=m^2_{\tilde{t}_R}+m_t^2+\frac{2}{3}\sin^2 \theta_W \cos(2\beta)m_Z^2,$$

$$m_{LR}=-\mu \cot \beta+\lambda_t, \tag{16}$$

where $m^2_{\tilde{t}_L}, m^2_{\tilde{t}_R}$ are the soft SUSY-breaking mass terms of left- and right-top squarks, μ is the coefficient of the H_1–H_2

mixing term in the superpotential, λ_t is the parameter describing the strength of soft SUSY-breaking trilinear scalar interaction $\tilde{t}_L\tilde{t}_R H_2$, and $\tan\beta = v_u/v_d$ is the ratio of the vacuum expectation values of the two Higgs doublets. In minimal supergravity models, the soft SUSY-breaking parameters $m^2_{\tilde{q}_L}$ and $m^2_{\tilde{q}_R}$ are equal to each other, so that the mass splitting $M^2_{\tilde{q}_L} - M^2_{\tilde{q}_R}$ is small, and of the same order of magnitude for all quark flavors. In this case, it is hard to expect observable asymmetries. On the other hand, in the general MSSM right- and left-squark masses $M_{\tilde{t}_{L,R}}$ are considered to be independent parameters, in which case there are no theoretical limitations on the splitting of top squark masses. In the following, the second point of view is accepted, so that $M_{\tilde{t}_R}$ is assumed to be of the order 90–175 GeV, while $M_{\tilde{t}_L}$ is varied between 150 and 1000 GeV.

The cross sections entering the asymmetry (6) are calculated in the usual way by convolution of the squared and spin- and color-averaged hard scattering matrix elements $|\mathcal{M}_{k_1k_2}|^2_{L,R}$ with the appropriate parton distributions $f_i(x)$:

$$\sigma(pp \to t_{L,R}\overline{t}) = \frac{\beta}{32\pi\hat{s}} \int_{-1}^{1} d\cos\theta \int dx_1 dx_2 \times \sum_{i_1,i_2} f_{i_1}(x_1) f_{i_2}(x_2) |\mathcal{M}^{i_1i_2}(\hat{s},\hat{t},\hat{u})|^2_{L,R}, \tag{17}$$

where $\hat{s},\hat{t},\hat{u}$ are the parton Mandelstam variables, $\beta \equiv \sqrt{1-4m_t^2/\hat{s}}$, and the particle momenta for the partons $q_{i_{1,2}}$ in the initial state are defined as $q_{i_1}(p_1) + q_{i_2}(p_2) \to t(p_3) + \overline{t}(p_4)$. The numerator of the asymmetry (6) is determined solely by the diagrams of Figs. 1(f), 1(g) (containing top squarks), which give the following matrix elements for the production of a left-handed top quark:

$$(\mathcal{M}_t\mathcal{M}_u^\dagger + \mathcal{M}_u\mathcal{M}_t^\dagger)_L = \sum_{i,j} \frac{a_i^2 a_j^2}{(\hat{t}-m^2_{\tilde{t}_i})(\hat{u}-m^2_{\tilde{t}_j})} \times \{4m_t^2\hat{s}(1-C_iC_j)[(1-C_iC_j)+(C_i-C_j)\cos\theta] - 2(m_t^2-\hat{t})(m_t^2-\hat{u})(1-C_i^2)(1-C_j^2)\}, \tag{18}$$

$$|\mathcal{M}_t|^2_L = \sum_{i,j} \frac{a_i^2 a_j^2}{2(\hat{t}-m^2_{\tilde{t}_i})(\hat{t}-m^2_{\tilde{t}_j})} (m_t^2-\hat{t})\hat{s}(1+C_iC_j) \times (A + B\cos\theta), \tag{19}$$

$$|\mathcal{M}_u|^2_L = \sum_{i,j} \frac{a_i^2 a_j^2}{2(\hat{u}-m^2_{\tilde{t}_i})(\hat{u}-m^2_{\tilde{t}_j})} (m_t^2-\hat{u})\hat{s}(1+C_iC_j) \times (A - B\cos\theta). \tag{20}$$

In these formulas

$$C_i \equiv \frac{b_i}{a_i}, \quad i=1,2, \tag{21}$$

$$A \equiv (1+C_i)(1+C_j)(1-\beta) + (1-C_i)(1-C_j)(1+\beta), \tag{22}$$

$$B \equiv (1+C_i)(1+C_j)(1-\beta) - (1-C_i)(1-C_j)(1+\beta), \tag{23}$$

the summation (i,j) goes over the two top squark masses. The squared matrix element $|\mathcal{M}^{\tilde{g}\tilde{g}}|^2_L$ entering Eq. (17) can be written in terms of Eqs. (18)–(20) as

$$|\mathcal{M}^{\tilde{g}\tilde{g}}|^2_L = \frac{1}{256}\left(\frac{16}{3}(|\mathcal{M}_t|^2 + |\mathcal{M}_u|^2) + \frac{2}{3}(\mathcal{M}_t\mathcal{M}_u^\dagger + \mathcal{M}_u\mathcal{M}_t^\dagger)\right)_L. \tag{24}$$

The matrix elements for the production of right-handed top quarks are obtained by the substitution

$$C_{i,j} \to -C_{i,j}. \tag{25}$$

If Eqs. (18)–(20) are combined with the explicit formulas (8) for a_i, b_i, it is possible to get the following expression for the difference of the matrix elements for producing the left- and right-handed top quarks in the $t\overline{t}$ pairs:

$$|\mathcal{M}^{\tilde{g}\tilde{g}}|^2_L - |\mathcal{M}^{\tilde{g}\tilde{g}}|^2_R = 4\cos 2\theta_t\{(X_{11}-X_{22})(\beta-\cos\theta) + (Y_{21}-Y_{12})\cos\theta + (Z_{11}-Z_{22})(\beta+\cos\theta)\}, \tag{26}$$

where

$$X_{ij} \equiv \frac{(m_t^2-\hat{t})\hat{s}}{96(\hat{t}-m^2_{\tilde{t}_i})(\hat{t}-m^2_{\tilde{t}_j})}, \tag{27}$$

$$Y_{ij} \equiv \frac{m_t^2\hat{s}}{192(\hat{t}-m^2_{\tilde{t}_i})(\hat{u}-m^2_{\tilde{t}_j})}, \tag{28}$$

$$Z_{ij} \equiv \frac{(m_t^2-\hat{u})\hat{s}}{96(\hat{u}-m^2_{\tilde{t}_i})(\hat{u}-m^2_{\tilde{t}_j})}. \tag{29}$$

Equation (26) depends on the mass mixing angle θ_t only through the common factor $\cos 2\theta_t$. This proves the argument given before that for fixed $m_{\tilde{t}_{1,2}}$ the asymmetry should be the largest at $m_{LR}=0$ and $\theta_t=-\pi/2$.

The diagrams in Figs. 1(a)–1(e) do not violate the parity and need to be included only in the denominator of the asymmetry (6). The matrix elements for the pure QCD processes [in Figs. 1(a)–1(d)] are well known, while the s-channel $\tilde{g}\tilde{g}$ diagram [in Fig. 1(e)] differs from the analogous $q\bar{q}$ one only by a color factor:

$$|\mathcal{M}^{q\bar{q}}|^2=\frac{4}{9}\,\frac{(m_t^2-\hat{t})^2+(m_t^2-\hat{u})^2+2m_t^2\hat{s}}{\hat{s}^2}, \tag{30}$$

$$\begin{aligned}|\mathcal{M}^{GG}|^2=\frac{1}{16}\Bigg(&\frac{(m_t^2-\hat{t})(m_t^2-\hat{u})}{12\hat{s}^2}+\frac{8}{3}\,\frac{(m_t^2-\hat{t})(m_t^2-\hat{u})-2m_t^2(m_t^2+\hat{t})}{(m_t^2-\hat{t})^2}+\frac{8}{3}\,\frac{(m_t^2-\hat{t})(m_t^2-\hat{u})-2m_t^2(m_t^2+\hat{u})}{(m_t^2-\hat{u})^2}\\&-\frac{2}{3}\,\frac{m_t^2(\hat{s}-4m_t^2)}{(m_t^2-\hat{t})(m_t^2-\hat{u})}-6\,\frac{(m_t^2-\hat{u})(m_t^2-\hat{t})+m_t^2(\hat{u}-\hat{t})}{\hat{s}(m_t^2-\hat{t})}-6\,\frac{(m_t^2-\hat{u})(m_t^2-\hat{t})-m_t^2(\hat{u}-\hat{t})}{\hat{s}(m_t^2-\hat{u})}\Bigg),\end{aligned} \tag{31}$$

$$|\mathcal{M}_s^{\tilde{g}\tilde{g}}|^2=\frac{27}{32}|\mathcal{M}^{q\bar{q}}|^2. \tag{32}$$

In the above, the spin and color factors in both the final and the initial states are all properly summed and averaged.

One can also obtain the total parton cross sections by the integration of Eqs. (18)–(20), (30)–(32) over the scattering angle θ. For the t and u channels we define

$$C\equiv 2(1-\beta^2)(1-C_iC_j)(C_i-C_j), \tag{33}$$

$$D\equiv \beta^2(1-C_i^2)(1-C_j^2), \tag{34}$$

$$E\equiv 2(1-\beta^2)(1-C_iC_j)^2-(1-C_i^2)(1-C_j^2), \tag{35}$$

$$v_i(\hat{s},\beta)\equiv\frac{2m_{\tilde{t}_i}^2+\hat{s}+\beta\hat{s}-2m_t^2}{2m_{\tilde{t}_i}^2+\hat{s}-\beta\hat{s}-2m_t^2}. \tag{36}$$

Then

$$[\sigma_{tu}^{\tilde{g}\tilde{g}}]_L=\sum_{i,j}\frac{g_s^4a_i^2a_j^2}{24576\pi}[8(1+C_iC_j)f_1(m_{\tilde{t}_i}^2,m_{\tilde{t}_j}^2)+f_2(m_{\tilde{t}_i}^2,m_{\tilde{t}_j}^2)], \tag{37}$$

$$\begin{aligned}f_1(m_{\tilde{t}_i}^2,m_{\tilde{t}_j}^2)=\frac{1}{\beta(m_{\tilde{t}_i}^2-m_{\tilde{t}_j}^2)}\Bigg(&-\frac{8B}{\hat{s}}\beta(m_{\tilde{t}_i}^2-m_{\tilde{t}_j}^2)\\&+4(m_{\tilde{t}_i}^2-m_t^2)(2Bm_{\tilde{t}_i}^2+B\hat{s}+A\beta\hat{s}-2Bm_t^2)/\hat{s}^2\,\ln v_i(\hat{s},\beta)\\&-4(m_{\tilde{t}_j}^2-m_t^2)(2Bm_{\tilde{t}_j}^2+B\hat{s}+A\beta\hat{s}-2Bm_t^2)/\hat{s}^2\,\ln v_j(\hat{s},\beta)\Bigg),\end{aligned} \tag{38}$$

$$\begin{aligned}f_2(m_{\tilde{t}_i}^2,m_{\tilde{t}_j}^2)=\frac{1}{\beta^2}\Bigg\{&-\frac{8D}{\hat{s}}\beta+\{[2E\beta^2\hat{s}^2+(4m_{\tilde{t}_i}^2+2\hat{s}-4m_t^2)(2Dm_{\tilde{t}_i}^2+D\hat{s}+C\beta\hat{s}-2Dm_t^2)]\\&\times\ln v_i(\hat{s},\beta)+[2E\beta^2\hat{s}^2+(4m_{\tilde{t}_j}^2+2\hat{s}-4m_t^2)(2Dm_{\tilde{t}_j}^2+D\hat{s}-C\beta\hat{s}-2Dm_t^2)]\ln v_j(\hat{s},\beta)\} \qquad (39)\\&\times\frac{1}{\hat{s}^2(m_{\tilde{t}_i}^2+m_{\tilde{t}_j}^2+\hat{s}-2m_t^2)}\Bigg\}.\end{aligned} \tag{40}$$

When $m_{\tilde{t}_i}=m_{\tilde{t}_j}$, we have

$$f_1(m_{\tilde{t}_i}^2=m_{\tilde{t}_j}^2)=\frac{1}{\beta}\Bigg\{-\frac{8B}{\hat{s}}\beta+4(4Bm_{\tilde{t}_i}^2+B\hat{s}+A\beta\hat{s}-4Bm_t^2)/\hat{s}^2\ \ln v_i(\hat{s},\beta)$$

$$+8(m_{\tilde{t}_i}^2-m_t^2)(2Bm_{\tilde{t}_i}^2+B\hat{s}+A\beta\hat{s}-2Bm_t^2)\left(\frac{1}{2m_{\tilde{t}_i}^2+\hat{s}+\beta\hat{s}-2m_t^2}-\frac{1}{2m_{\tilde{t}_i}^2+\hat{s}-\beta\hat{s}-2m_t^2}\right)\Bigg/\hat{s}^2\Bigg\}. \quad (41)$$

Again, $[\sigma_{tu}^{\tilde{g}\tilde{g}}]_R$ can be obtained by the substitution

$$C_i\rightarrow -C_i, C_j\rightarrow -C_j. \quad (42)$$

The cross sections of the other subprocesses, corresponding to Eqs. (30)–(32), are given by

$$\sigma^{q\bar{q}}=\frac{g_s^4}{108\pi\hat{s}}\beta(2+\rho), \quad (43)$$

$$\sigma^{GG}=\frac{g_s^4}{48\pi\hat{s}}\left[\left(1+\rho+\frac{\rho^2}{16}\right)\ln\frac{1+\beta}{1-\beta}-\beta\left(\frac{7}{4}+\frac{31}{16}\rho\right)\right], \quad (44)$$

$$\sigma_s^{\tilde{g}\tilde{g}}=\frac{g_s^4}{128\pi\hat{s}}\beta(2+\rho), \quad (45)$$

where $\rho\equiv 4m_t^2/\hat{s}$.

IV. NUMERIC RESULTS

To estimate the largest possible asymmetries, we varied the squark mass eigenvalues $m_{\tilde{t}_{1,2}}$ with m_{LR} set to be zero (see the discussion in the previous section). No assumption was made about any model-specific relationships between the values of the mass parameters $M_{\tilde{t}_{L,R}}$ and m_{LR} [cf. Eq. (16)].

If $m_{LR}=0$, the left-right-handed quarks couple independently to the left-right-top squarks. Correspondingly, for $m_{\tilde{t}_1}\neq m_{\tilde{t}_2}$, the production rates of the left- and right-handed top quarks will be different. The asymmetry A_t is expected to grow when the mass splitting $m_{\tilde{t}_1}\neq m_{\tilde{t}_2}$ increases. In this work, the asymmetries were calculated for $m_{\tilde{t}_1}=90$ GeV (which is consistent with the current LEP2 data [7]), $m_{\tilde{t}_1}=m_t=175$ GeV, and various values of $m_{\tilde{t}_2}$. Two values of factorization scale $\mu=m_t$ and $2m_t$ were used. Various sets of masses will be further denoted as $(m_{\tilde{t}_1},m_{\tilde{t}_2},m_{LR})$, with

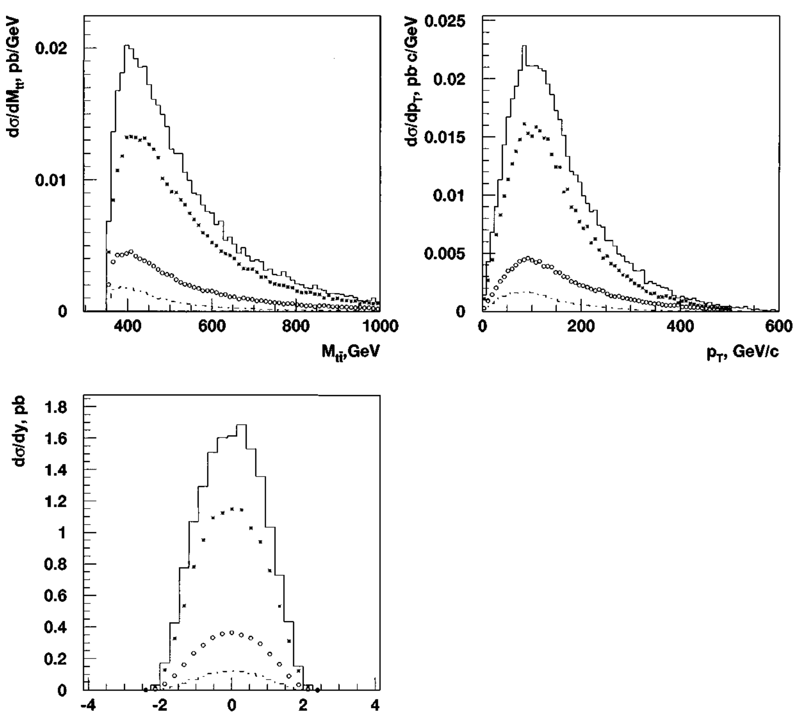

FIG. 2. The dependence of the cross section of $t\bar{t}$ pair production on various kinematic parameters: $t\bar{t}$ pair invariant mass $M_{t\bar{t}}$, t-quark transverse momentum p_T, and rapidity y. The solid line, stars, circles, and dashed line correspond to the full differential cross section and the contributions of gluon, quark, and gluino subprocesses, respectively. The factorization scale $\mu=2m_t$, and the squark masses are (90,1000,0).

numerical values in GeV. As before, the gluino mass is assumed to be equal to 0.5 GeV.

In the SM, both t and $\overline{t}$ decay into $b(\overline{b})$ and $W^{\pm}$ with a probability of almost unity, with a subsequent decay of the W bosons into two jets or two leptons. In the MSSM, when both the gluino and the top squark are light, the top quark can also decay via $t\rightarrow\widetilde{g}\widetilde{t}_1$, so that the branching ratio of $t\rightarrow W^{+}+b$ decreases. Assuming that all the other supersymmetric particles are heavier than the top quark, and $\theta_t=-\pi/2$, the branching ratio for $t\rightarrow W^{+}+b$ is equal to 0.29 and 1 for $m_{\tilde{t}_1}=90$ and 175 GeV, respectively. The Collider Detector at Fermilab (CDF) collaboration has measured the branching ratio of $t\rightarrow W^{+}+b$ to be $0.87^{+0.13+0.13}_{-0.30-0.11}$ [22]. Hence, the chosen sets of the values for $m_{\tilde{t}_1}$ and $m_{\tilde{g}}$ are still allowed by data within 95% C.L.

It is convenient to study the asymmetry A_t using the semileptonic modes of decay, with $t\rightarrow bl^{+}\nu_l$ $(l=e,\mu)$ and $\overline{t}\rightarrow\overline{b}q\overline{q}$ (or vice versa), which have a branching ratio of about 0.086 and 24/81 for $m_{\tilde{t}_1}=90$ and 175 GeV, respectively. In the following we assume that it will be possible to reconstruct the kinematics of a $t\overline{t}$ pair from the momenta of the decay products by requiring the transverse momenta $p_T^{\mathrm{jets}}\geqslant 30$ GeV, $p_T^{\mathrm{leptons}}\geqslant 20$ GeV, $e_T\geqslant 20$ GeV, the rapidities of the jets and leptons $|y|<2.0$, and the jet cone separation $\Delta R>0.4$ [23]. We also assume that it will be necessary to tag one b quark with an efficiency $C_b=50\%$. We estimate the statistical error in the measurement of the asymmetry by

$$\delta A_t=\frac{1}{\sqrt{\mathcal{L}TC_b(\sigma_L^{\mathrm{tot}}+\sigma_R^{\mathrm{tot}})}}, \tag{46}$$

where we assume the observation time $T=1$ yr and the luminosity $\mathcal{L}=100\ \mathrm{fb}^{-1}/\mathrm{yr}$, corresponding to the second run of the LHC.

The imposed selection cuts and branching ratio significantly reduce the total cross section of $t\overline{t}$ production, typi-

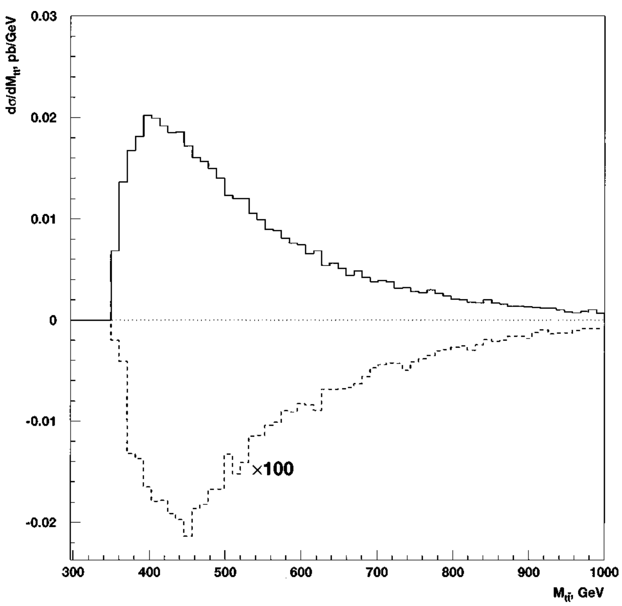

FIG. 3. Dependence of the sum $d\sigma_L/dM_{t\overline{t}}+d\sigma_R/dM_{t\overline{t}}$ (solid line) and the difference $d\sigma_L/dM_{t\overline{t}}-d\sigma_R/dM_{t\overline{t}}$ (dashed line, magnified by 100) of the differential cross sections of the production of left- and right-handed top quarks on the invariant mass of $t\overline{t}$ pairs $M_{t\overline{t}}$. The factorization scale $\mu=2m_t$, and the squark masses are (90,1000,0).

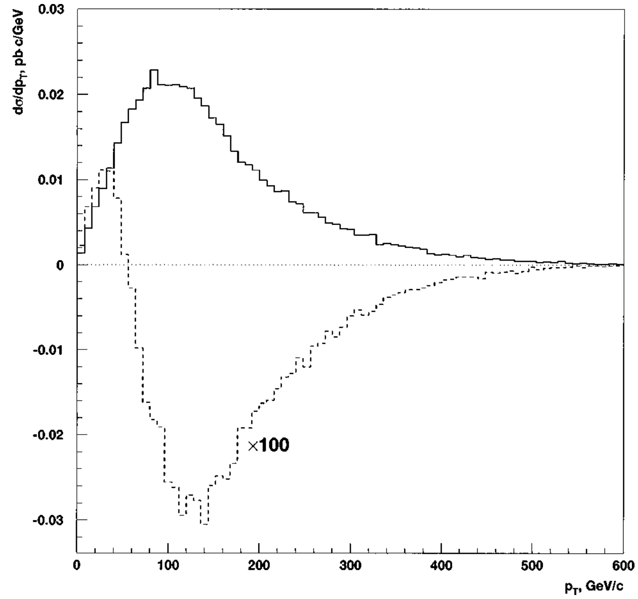

FIG. 4. Dependence of the sum $d\sigma_L/dp_T+d\sigma_R/dp_T$ (solid line) and the difference $d\sigma_L/dp_T-d\sigma_R/dp_T$ (dashed line, magnified by 100) of the differential cross sections of the production of the left- and right-handed top quarks on the transverse momentum of the t quark p_T. The factorization scale $\mu=2m_t$, and the squark masses are (90,1000,0).

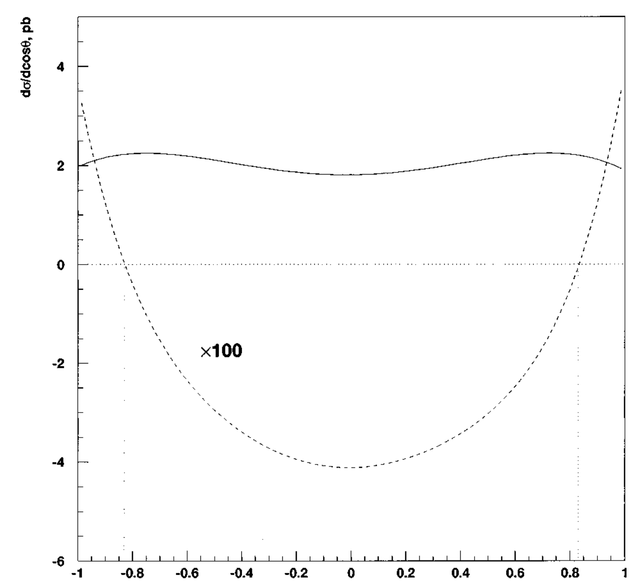

FIG. 5. Dependence of the sum $d\sigma_L/d\cos\theta+d\sigma_R/d\cos\theta$ (solid line) and the difference $d\sigma_L/d\cos\theta-d\sigma_R/d\cos\theta$ (dashed line, magnified by 100) of the differential cross sections of the production of left- and right-handed top quarks on the cosine of the scattering angle in the $t\overline{t}$ pair rest frame. The factorization scale $\mu=2m_t$, and the squark masses are (90,1000,0).

TABLE I. The asymmetries A_t (in %) predicted by SUSY QCD, and the estimated statistical errors of their measurement δA_t for the LHC luminosity $\mathcal{L}=100$ fb^{-1}/yr. Blank entries correspond to asymmetries which are too small to be observed.

	$\mu=m_t$				$\mu=2m_t$			
Masses (GeV)	$\lvert\cos\theta\rvert\leqslant 0.8$		$\lvert\cos\theta\rvert>0.8$		$\lvert\cos\theta\rvert\leqslant 0.8$		$\lvert\cos\theta\rvert>0.8$	
$(m_{\tilde{t}_1},m_{\tilde{t}_2},m_{LR})$	A_t	δA_t	A_t	δA_t	A_t	δA_t	A_t	δA_t
(90,150,0)	−0.31	0.23	1.14	0.54	−0.35	0.25	1.20	0.60
(90,200,0)	−0.57	0.23	1.30	0.54	−0.62	0.25	1.42	0.60
(90,500,0)	−1.31	0.23	1.20	0.54	−1.39	0.25	1.33	0.60
(90,1000,0)	−1.50	0.23	1.05	0.54	−1.61	0.25	1.20	0.60
(175,250,0)	−0.33	0.13			−0.36	0.14		
(175,500,0)	−0.86	0.13			−0.91	0.14		
(175,1000,0)	−1.04	0.13			−1.11	0.14		

cally from around 340 pb down to 3.5 and 12 pb for $m_{\tilde{t}_1}=90$ and 175 GeV, respectively. As an example, Fig. 2 shows various differential cross sections including the GG, $q\bar{q}$, and $\tilde{g}\tilde{g}$ subprocesses for the squark masses (90,1000,0) and $\mu=2m_t$, obtained with the kinematic cuts and branching ratios applied. It can be readily seen that the dominant part of the $t\bar{t}$ pairs is produced due to the gluon-gluon subprocess, which contributes around 71% of the total rate. The quark-antiquark and gluino-gluino shares are 22 and 7%, respectively. The gluino contribution is comparable with the conventional QCD uncertainties in the knowledge of the total rate (about 5 to 10%), however, the presence of the light gluino will change the shape of the cross-section distributions. Thus, in principle there is a possibility to detect the light gluino by carefully fitting the event rate distributions and comparing them with the predictions of perturbative QCD.

Figure 3 shows the sum of the differential cross sections of left- and right-handed top quarks production $d\sigma_L/dM_{t\bar{t}}+d\sigma_R/dM_{t\bar{t}}$, and their difference $d\sigma_L/dM_{t\bar{t}}-d\sigma_R/dM_{t\bar{t}}$ (scaled by a factor of 100), as functions of the invariant mass of the $t\bar{t}$ pair $M_{t\bar{t}}$. One can see that the asymmetry is most noticeable in the region of small and intermediate values of $M_{t\bar{t}}$. This is different than the behavior of the asymmetry produced due to the presence of superpartners in the loop corrections [19]. In that case, the asymmetry becomes significant in the region of large $M_{t\bar{t}}$, where in the case of the light gluino it can have a value of 2–3%. In this respect, we expect the minimal interference between the tree-level and loop-generated asymmetries, since the main contributions to them come from different kinematic regions.

The dependence of the cross sections on two other kinematic parameters, the transverse momentum of the t quark and the cosine of the scattering angle in the $t\bar{t}$ rest frame, is shown in Figs. 4 and 5. As can be seen from Fig. 5, the difference $d\sigma_L/d\cos\theta-d\sigma_R/d\cos\theta$ changes its sign around $\cos\theta\approx\pm 0.8$, so that one can enhance the asymmetry by separately considering the cross sections integrated over either large or small angles. It can also be shown that the asymmetries at small angles can be further enlarged by rejecting the events with transverse momenta larger than 100 GeV/c. For the other combinations of top squark masses, $d\sigma_L/\cos\theta-d\sigma_R/\cos\theta$ changes its sign at slightly lower $|\cos\theta|$, approximately 0.75–0.8. We therefore present the asymmetries of the cross sections integrated separately over the region $|\cos\theta|\leqslant 0.8$, or the region $|\cos\theta|>0.8$ with $p_T\leqslant 100$ GeV/c.

Table I shows the values of the asymmetry A_t obtained after the integration of the rate with the aforementioned cuts in $|\cos\theta|$ and p_T. As can be seen from the table, for various top squark masses the asymmetry ranges from 0.3 to 1.1%. The behavior of the asymmetries with the growth of $m_{\tilde{t}_2}$ is different at large and small angles. At $|\cos\theta|\leqslant 0.8$ the asymmetry monotonously increases with the growth of $m_{\tilde{t}_2}$, while at $|\cos\theta|>0.8$ the asymmetry has a maximum around $m_{\tilde{t}_2}=200$ GeV and then starts to decrease. At small angles ($|\cos\theta|\leqslant 0.8$) the asymmetry quickly decreases with the growth of the mass of the lighter squark and becomes practically unnoticeable for $m_{\tilde{t}_1}\geqslant m_t$.

For the comparison, we also give in the same table the statistical errors δA_t from Eq. (46). These errors are mostly determined by GG and $q\bar{q}$ cross sections, so that they hardly depend on the choice of the squark masses. For most combinations of the top squark masses, the obtained values of A_t can in principle be distinguished from the statistical error δA_t at a 2σ level or better. However, what can be more important are the experimental systematic uncertainties related to the measurement of the asymmetries of the order 1%. In particular, it can be challenging to reach the necessary accuracy in the reconstruction of the kinematics of the $t\bar{t}$ pair, and the determination of the top quark polarization. Nevertheless, the predictive power of this analysis can be increased if it is combined with the search for the signature of the light gluinos in other kinematic regions, for instance, for loop-generated asymmetries in the production of top-antitop pairs with large invariant masses.

V. CONCLUSION

In this work we proposed a new method based on the search for possible violations of discrete symmetries of the standard model, to test the existence of a light gluino in the MSSM. This is in contrast with many other methods presented in the literature (see the Introduction), in which one has to assume how a light gluino hadronizes into hadron states to be compared with the experimental measurement.

We study the consequences the small mass of the gluino would have for the production of top quarks at the LHC via the tree-level process $\tilde{g}\tilde{g}\rightarrow t\bar{t}$. We show that with a large mass splitting in the masses of superpartners (top squarks) of the top quark, the gluino-gluino fusion process can generate the parity-violating asymmetry in the production of left- and right-handed t quarks. Since SM QCD theory preserves the discrete symmetry of P parity, a small violation of such a symmetry may be observed from a large $t\bar{t}$ data sample at the LHC.

For $m_{\tilde{g}}\approx 0$ the largest values of the parity-violating asymmetry discussed in the previous sections is around 0.3–1.1% for various choices of SUSY parameters. Hence, it can in principle be observed, taking into account the high rate of top quark production at the LHC. In order to measure the asymmetry with a small statistical error, the experiment should be preferably done during the second run of LHC with an integrated luminosity of 100 fb^{-1}/yr. The rate of the top quark production does not seem to be the major obstacle for the measurement of the parity-violating asymmetry. However, it demands a good understanding of the systematic errors, better than 1%, to reach the precision of the measurement sufficient to test the existence of a light gluino in $t\bar{t}$ pair production.

ACKNOWLEDGMENTS

We would like to thank L. Clavelli, L. Dixon, G. R. Farrar, H. L. Lai, R. Raja, T. Rizzo, C. Schmidt, Z. Sullivan, and W.-K. Tung for helpful discussions. This work was supported in part by the National Natural Science Foundation of China, a grant from the State Commission of Science and Technology of China, and by the U.S. NSF Grant No. PHY-9507683.

[1] H. E. Haber and G. L. Kane, Phys. Rep. **117**, 75 (1985); J. F. Gunion and H. E. Haber, Nucl. Phys. **B272**, 1 (1986).
[2] For a recent review, see J. Gunion, in *Proceedings of the International Workshop in Quantum Effects in the Minimal Supersymmetric Standard Model*, Barcelona, 1997, edited by J. Sola, Report No. UCD-98-2, hep-ph/9801417.
[3] R. Barbieri, L. Girardello, and A. Masiero, Phys. Lett. **127B**, 429 (1983); G. Farrar and A. Masiero, Report No. RU-94-38, hep-ph/9410401; G. Farrar, Nucl. Phys. B (Proc. Suppl.) **62**, 485 (1998).
[4] ALEPH Collaboration, R. Barate *et al.*, Z. Phys. C **76**, 1 (1997).
[5] G. R. Farrar, in *Proceedings of the 11th Les Rencontres de Physique de la Vallee d'Aoste: Results and perspectives in particle physics*, La Thuile, Italy, 1997, edited by Mj. Greco, p. 779, Report No. RU-97-22, hep-ph/9707467.
[6] F. Csikor and Z. Fodor, Phys. Rev. Lett. **78**, 4335 (1997); Report No. ITP-Budapest 538,KEK-TH-551, hep-ph/9712269.
[7] P. Wells, in Proceedings of the 8th LEP Performance Workshop, Chamonix, 1998 (unpublished); PDF version available at URL http://www.cern.ch/CERN/Divisions/SL/publications/index.html
[8] S. Raby, Phys. Rev. D **56**, 2852 (1997); R. N. Mohapatra and S. Nandi, Phys. Rev. Lett. **79**, 181 (1997).
[9] G. Farrar, Report No. RU-95-25, hep-ph/9508291.
[10] KTeV Collaboration, J. Adams *et al.*, Phys. Rev. Lett. **79**, 4083 (1997).
[11] Farrar [3].
[12] J. L. Hewett, T. G. Rizzo, and M. A. Doncheski, Phys. Rev. D **56**, 5703 (1997); L. Clavelli, and I. Terekhov, Phys. Lett. B **385**, 139 (1996); I. Terekhov, *ibid.* **412**, 86 (1997).
[13] J. Blümlein and J. Botts, Phys. Lett. B **325**, 190 (1994); **331**, 449(E) (1994).
[14] R. Rückl and A. Vogt, Z. Phys. C **64**, 431 (1994).
[15] H1 Collaboration, S. Aid *et al.*, Nucl. Phys. **B439**, 471 (1995); **B470**, 3 (1996).
[16] ZEUS Collaboration, M. Derrick *et al.*, Z. Phys. C **65**, 379 (1995); **72**, 399 (1996).
[17] NMC Collaboration, M. Arneodo *et al.*, Phys. Lett. B **364**, 107 (1995).
[18] C. Kao, G. Ladinsky, and C.-P. Yuan, Int. J. Mod. Phys. B **12**, 1341 (1997); C. Kao, Phys. Lett. B **348**, 155 (1995).
[19] Chong Sheng Li, C.-P. Yuan, and Hong-Yi Zhou, Phys. Lett. B **424**, 76 (1998).
[20] CTEQ Collobaration, H. L. Lai *et al.*, Phys. Rev. D **55**, 1280 (1997).
[21] I. Antoniadis *et al.*, Nucl. Phys. **B211**, 216 (1983).
[22] CDF Collaboration, J. Incandela *et al.*, Nuovo Cimento A **109**, 741 (1996).
[23] ATLAS technical proposal, Report No. CERN/LHCC/94-43.